



Poly (glycerol sebacate) and polyhydroxybutyrate electrospun nanocomposite facilitates osteogenic differentiation of mesenchymal stem cells

Mohammad Foad Abazari^{a,1}, Shohreh Zare Karizi^{b,1}, Hadi Samadian^c, Navid Nasiri^d, Hassan Askari^e, Matin Asghari^f, Fateme Frootan^g, Hadi Bakhtiari^h, Hossein Mahboudiⁱ, Vahid Mansouri^{j,*}

^a Research Center for Clinical Virology, Tehran University of Medical Sciences, Tehran, Iran

^b Department of biology, Varamin Pishva Branch, Islamic Azad University, Pishva, Varamin, Iran

^c Nano Drug Delivery Research Center, Health Technology Institute, Kermanshah University of Medical Sciences, Kermanshah, Iran

^d Institute of Molecular Biology, Vrije Universiteit Brussel, Brussels, Belgium

^e Gastroenterohepatology Research Center, Shiraz University of Medical Sciences, Shiraz, Iran

^f Department of Molecular Biotechnology, Cell Science Research Center, Royan Institute of Biotechnology, ACECR, Isfahan, Iran

^g Institute of Agricultural Biotechnology, National Institute of Genetic Engineering & Biotechnology (NIGEB), Tehran, Iran

^h Department of Clinical Biochemistry, School of Pharmacy and Pharmaceutical Sciences, Isfahan University of Medical Sciences, Isfahan, Iran

ⁱ Department of Biotechnology, School of Pharmacy, Alborz University of Medical Sciences, Karaj, Iran

^j Proteomics Research Center, Faculty of Paramedical Sciences, Shahid Beheshti University of Medical Sciences, Tehran, Iran

ARTICLE INFO

Keywords:

Poly (glycerol sebacate)
Polyhydroxybutyrate
Electrospinning
Bone
Nanofibers

ABSTRACT

Bone tissue engineering is a rapidly growing approach for repairing bone lesions, which needs scaffolds that meet biomechanical and bio-structural requirements of target tissues. The aim of the present study is to demonstrate the potential application of fabricated poly (glycerol sebacate) and Polyhydroxybutyrate (PGS-PHB) nanofibrous scaffold by electrospinning, as a potential bone implant. Herein, after morphological study by SEM, the biological behavior and toxicity of the constructed scaffold were evaluated by cell attachment, protein adsorption and MTT assay. Then the supportive potential of the scaffold upon osteogenic differentiation process was investigated by the culture of adipose tissue-derived mesenchymal stem cells (ADSCs). The results showed that the PGS-PHB scaffold was nanofibrous, with a uniform surface and good porosity. The protein adsorption capacity of the scaffold was significantly higher than tissue culture plate (TCP) as a control group. The initial cell attachment in the PGS-PHB scaffold and TCP was not significantly different. Finally, the osteogenic differentiation potential of the ADSCs cultured on the PGS-PHB scaffold and TCP were evaluated by assessment of alkaline phosphatase (ALP) activity, calcium content and bone-related gene expression. The results revealed that the ALP activity, calcium producing and expression level of bone-related genes in the cultured cells in the PGS-PHB scaffold group was significantly higher than cultured cells in the control group. Based on the obtained results, the constructed PGS-PHB scaffold has promising potential for use in bone tissue engineering applications.

1. Introduction

Bone tissue plays an important role in the body, so any fundamental change or disease in its structure, which may occur as a result of an accident, various diseases and wounds, affects the balance of the body and the nature of a person's life [1]. Fortunately, the most bone damage

in the body, heals on its own with minimal intervention. But others do not heal on their own for a variety of reasons, such as misplaced bone fusion, complete bone loss from a tumor, or infection at the site of the lesion [2,3]. In such cases, various methods such as bone grafting (autologous or allogeneic) or metal implants are used to completely repair the bone [4,5]. Although autograft is the gold standard for bone

* Corresponding author.

E-mail address: V.Mansouri@sbm.ac.ir (V. Mansouri).

¹ Authors contributed equally at this work.

grafting, its limited resources have made its use impractical, especially in large bone lesions. In addition, bone removal procedures are associated with the risk of infection and also require secondary surgery. In addition to the risk of infection, the use of allogeneic bone grafts also increases the risk of rejection [6]. Alternative treatment has usually been the use of metal implants, the accumulation of metallic implants in various organs can be associated with the release of harmful ions in the body and thus increase the risk of cancer [7].

For this reason, in recent decades, researchers focused their efforts on finding new materials to prevent these problems, which has led to the introduction of bone tissue engineering [8–10]. Tissue engineering design scaffolds using biodegradable biomaterials with the proper physical structure according to the target tissues. These scaffolds ultimately support adhesion, growth, proliferation and differentiation of the cells and allow the damaged section to regenerate or produce new tissues [11–14]. Scaffolds can be fabricated in a single polymer, a combination of polymers, a combination of polymers and bioceramics, and/or a combination of polymers and growth factors or bioactive molecules, using different methods [15–18].

Poly (hydroxybutyrate) (PHB) is a type of Polyhydroxyalkanoates (PHAs) polymers used in tissue engineering, because PHB is compatible with blood and mammalian tissues [19]. PHB monomer is a natural metabolite in human blood. Because the body reabsorbs PHB, it is used in surgery as a suture to heal wounds and blood vessels. In pharmacy, PHB can also be used as a microcapsule in therapy or as a cell pack and a tablet [20]. Due to its piezoelectric property, PHB has the ability to regenerate bone, which is why many studies have used the combination of this polymer with other polymers and ceramics, such as PLLA [21], nano hydroxyapatite (nHA) [22,23], Bioactive-glass [24], Tricalcium Phosphate [25], and etc. These properties alone are not enough for bone tissue engineering, for this reason, copolymerization of PHB with other biodegradable synthetic polymers, such as polyglycerol sebacate (PGS) can be a good option for fabricating nanofibrous scaffolds to accelerate bone repair and regeneration. PGS has controllable mechanical, chemical and degradation properties and was introduced for use in tissue engineering [26]. Although PGS nanofibers have not been used so far in bone tissue engineering, other forms of PGS scaffolds such as film and sponge alone and in combination with nHA, PEG and etc. have been used in bone tissue engineering [27–31].

In the present study, PGS-PHB nanofibrous scaffold was fabricated by electrospinning. After structural and morphological characterization, adipose tissue-derived mesenchymal stem cells (ADSCs) were cultured on the PGS-PHB nanofibers and stem cells osteogenic differentiation potential were investigated by common osteogenic markers. This is the first study to attempt the promotion of osteogenesis by applying PGS-PHB composite nanofibers.

2. Materials and methods

2.1. Scaffold fabrication

Electrospinning was applied to fabricating of the PGS-PHB nanofibrous scaffold. CHCl₃ (25% w/v) was applied to dissolving PHB granules (1001MD, BASF). For synthesizing PGS prepolymer based on the previously reported method [32], 0.1 M polyol glycerol (BioXtra, 99%, Sigma Aldrich, Munich, Germany) and 0.1 M sebacic acid (99%, Sigma Aldrich, Munich, Germany) were blended with a molar stoichiometric ratio of 1:1 and stirred at 120 °C in a nitrogen atmosphere for 24 h and pressure less than 50 mTor. PGS-PHB solution was also prepared by enhancing the needed amounts of PGS (30 wt%) to the prepared PHB solution at room temperature while placed on the magnetic stirrer for 24 h. Then, the prepared PGS-PHB solution was purged to a 10 ml glass syringe and then placed in the electrospinning machine. The electrospinning parameters were considered as 15 kV for applied voltage, 11 cm for distance of needle with collector, 1.1 ml/h for flow rate of the solution, 25 °C for inside temperature of the machine and a

relative humidity of 43 ± 5%. Fabricated scaffolds were cut circularly in 14.00 mm diameter (area = 1.53 cm²). After that, Scaffolds were inserted in the 24-well plates and sterilized by UV irradiation (30 min) and filtered ethanol (1 h) at room temperature and then all experiments were performed in the 24-well plates.

2.2. Scaffold characterization

2.2.1. Protein adsorption

Protein adsorption was measured according to the previously reported protocol [33], in brief, solution-I (phosphate buffered saline (PBS) (10 mM, pH 7.4), fetal bovine serum (FBS) (1% v/v)) was added to the TCP and PGS-PHB scaffold for 1 h at room temperature. After that, supernatants were removed and then solution-II (PBS, 2.0 wt% SDS) was added to the TCP and PGS-PHB scaffold for 20 h to releasing the proteins attached to their surfaces. Total protein content of solution-II was measured using PARS-AZMOON total protein kit (Tehran, Iran) and a micro-plate reader (BioTek, USA) at 530 nm according to the manufactured protocol. The mean of adsorbed proteins reported in µg/mm³ of samples measured from a solution-III (BSA calibration in 2.0 wt% SDS in 10 mM PBS).

2.2.2. Scanning electron microscopy

Scanning electron microscopy (SEM) was applied to morphological characterization of the fabricated scaffold before and after cell seeding. The small pieces of the scaffolds were placed on the aluminum stubs and then a thin layer of gold sputtered over the surface of the scaffolds. But, for those cell seeded on their surface, before placed on the aluminum stubs, scaffolds were fixed by 2.5% glutaraldehyde (Sigma Aldrich, St. Louis, MO) and then dehydrated by adding of filtered ethanol (50°–100°). Finally scaffolds were visualized using a SEM (KYKY, EM3200, China) at an accelerating voltage of 20 kV.

2.2.3. In vitro degradation

Fabricated PGS-PHB scaffolds in a certain dimension (1.53 cm²) were weighed (W₀), and then inserted into 5 ml of basal medium (DMEM supplemented with 10% FBS) while incubated at 37 °C for 30 days. Every three days, three scaffolds were removed and then washed with distilled water and vacuum dried. Dried samples were weighed again (W_d). Weight loss (WL%) was obtained by the following equation: {WL = ((W_d-W₀)/W₀) 100%}.

2.2.4. Cell attachment and viability assays

MTT assay was performed to evaluate cell attachment and adipose derived mesenchymal stem cells (ADSCs) viability when grown on the PGS-PHB scaffold and tissue culture plate (TCP). On the certain time points, culture medium was removed and MTT solution (5 mg/ml) was added to the each sample at 8 h for cell attachment assay and days 1, 3, 5, 7 and 10 for viability assay. Samples contained MTT solution were incubated at 37 °C, 5% CO₂ for 4 h. After that, medium was removed and scaffolds were transferred to the new 24-well plate, and then formed formazan crystals at the bottom of the culture plated and on the scaffolds were dissolved using DMSO (Merck, Germany) while shaking gently for 10 min. Finally, supernatants were collected and read using a micro-plate reader (BioTek Instruments, USA) at 570 nm.

2.3. Cell culture

ADSCs were purchased from SCRTC stem cell bank (Tehran, Iran) [34]. To confirm stem cells differentiation potential, ADSCs at passage 2 were cultured under osteogenic medium (DMEM, 10% FBS, 10 µM beta-glycerol phosphate, 100 µM dexamethasone and 50 µM ascorbic acid (all from Sigma-Aldrich, USA) and adipogenic medium (DMEM, 10% FBS, dexamethasone 1 µM, insulin 1.7 µM, indomethacin 200 µM and IBMX 500 µM (all from Sigma-Aldrich, USA). After two weeks, paraformaldehyde 4% was added to the samples for 45 min while

incubated at 4 °C. Then samples were washed very slowly using cold PBS. Cultured ADSCs under osteogenic medium were stained with alizarin red (Behnogen, Iran) for 5 min, and those cultured under adipogenic medium were stained with Oil red (Merck, Germany) for 10 min. For DAPI staining, the cells cultured on the PGS-PHB scaffold were fixed using paraformaldehyde 4% on day 10 after cell seeding while incubated at 4 °C for 45 min. After that, fixator was removed and then DAPI was added to the samples for 1 min, and then supernatant was removed and samples were washed again for two times. Finally, stained samples were visualized using an inverted light microscope.

ADSCs were cultured on the fabricated PGS-PHB scaffold and TCP with a cell density of 10^4 per cm^2 and 5×10^3 per cm^2 under basal medium (DMEM and 10% FBS) for cell attachment and viability assays, respectively. For differentiation evaluation, ADSCs were cultured on the fabricated PGS-PHB scaffold and TCP with a cell density of 3×10^4 per cm^2 under differentiation medium.

2.4. Alkaline phosphatase activity

For ALP activity assessment, RIPA cell lysis buffer was added to the samples while shaking gently at 4 °C for 4 h. After that, samples were centrifuged at 15000 RPM at 4 °C for 15 min for total protein extraction. Reagents in PARS-AZMOON ALP and total protein kits (Tehran, Iran) were added to the collected supernatants and their optical densities were read using a micro-plate reader (BioTek Instruments, USA) at 405 nm. Obtained ALP activities were normalized in comparison with total protein using a BCA Protein Assay Kit (Pierce, Bonn, Germany).

2.5. Calcium content

For total calcium measurement, 0.6 N HCL (Merck, Germany) was added to the samples while shaking for 1 h. After that, supernatants were collected and their optical densities at 570 nm were obtained by adding of a reagent of PARS-AZMOON calcium content kit (Tehran, Iran). The calcium amounts were normalized in comparison with a standard curve obtained from optical densities of pure calcium serial dilution.

2.6. Real-time RT-PCR

The expression fold changes of ALP, Runt-related transcription factor 2 (Runx2), Osteonectin, Collagen type 1 (COL1) and Osteocalcin were assessed using real time RT-PCR. On days 7 and 14 after cell seeding, ADSCs cultured on the TCP and fabricated PGS-PHB nanofibrous scaffold were detached by trypsin and then Qiazol (Qiagen) was added to the cells for total RNA extraction. Then, random-hexamers (Vivantis) and Reverse Transcriptase (Vivantis Cat No: RTPL12) were used for synthesizing cDNA. The PCR parameters were included, 95 °C for denaturation (3 min), 95 °C, 40 cycles of 20 s, 60 °C for annealing (30 s) and 72 °C for elongation (30 s). Finally, SYBR Premix-Ex-Taq Master-mix (Takara, Japan) and designed primers (Table 1) using a StepOne Plus thermocycler (Applied Biosystems, Foster City, CA) were applied in real

Table 1

Primer sequences which used at this study.

| Gene | Primer sequences | Size (bp) |
|---|---|-----------|
| β -2-Micro globulin (β 2M) | TGGAAGAAGATACCAAATATCGA GATGATTCAGAGCTCCATAGAGCT | 201 |
| Collagen I | TGGAGCAAGAGGCGAGAG CACCAGCATCACCTTAGC | 121 |
| Runx2 | GCCTTCAAGGTGGTAGCCC CGTTACCCGCCATGACAGTA | 66 |
| Osteonectin | AGGTATCTGTGGGAGCTAATC ATTGCTGCACACCTTCTC | 224 |
| Osteocalcin | GCAAAGTGCAGCCTTTGTG GGCTCCAGCCATTGATACAG | 80 |
| ALP | GCACCTGCCTACTAACT C AGACACCCATCCCATCTC | 161 |

time RT-PCR, while β -2-Micro globulin (β 2 M) was considered as an internal control.

2.7. Statistical analysis

All experimental data are illustrated as mean \pm standard deviation of the mean. One-way analysis of variance (ANOVA) (SPSS software, version 17.0, Chicago, IL, USA) was used to analyze statistical differences between the experimental groups with $p < 0.05$.

3. Results

3.1. Cell culture

Homogeneous fibroblast-like cells with spindle shape were observed at passage two (Fig. 1A). To evaluate the differentiation potential of the ADSCs, cells were cultured under adipogenic and osteogenic mediums for two weeks and then stained by oil red (Fig. 1B) and alizarin red (Fig. 1C), respectively. Results demonstrated that ADSCs were differentiated properly to the adipocyte-like cells and osteoblast-like cells by detecting mineralization and oil vesicles as important adipogenic and osteogenic related markers, respectively.

3.2. Scaffold characterization

Fabricated PGS-PHB nanofibrous scaffolds were characterized morphologically using SEM and results demonstrated that the scaffolds were fibrous with smooth, bead free and nano-scale fibers (300 ± 200 nm), and also with interconnected pores (Fig. 2A). The cell attachment assay was performed by culture of ADSCs on the surface of the PGS-PHB nanofibrous scaffold and TCP as a control. The results indicated that adhered cells on the surface of the PGS-PHB nanofibers and TCPS were not significantly different (Fig. 2B). In addition, the amount of protein adsorption that could play a key role in cells adhering to the substrate was evaluated. The results demonstrated that the amount of adsorbed protein on the surface of PGS-PHB nanofibers was significantly higher than adsorbed protein on the surface of the TCP (Fig. 2C). Degradation assay was carried out for PGS-PHB fabricated scaffold *in vitro*, and the results revealed that only 25–26% of the PGS-PHB nanofibrous scaffold was degraded during 30 days (Fig. 2D). Scaffold's non-toxicity was qualitatively studied using SEM. The images taken on the tenth day after cell seeding showed that the ADSCs had almost completely covered the surface of the PGS-PHB nanofibrous scaffold (Fig. 3A). DAPI staining was also performed to confirm the presence of cells on the constructed scaffolds (Fig. 3B). Attachment of the ADSCs on the surface of the TCP as a control group was also depicted by light microscope (Fig. 3C) and florescent microscope after staining with DAPI (Fig. 3D). Nan-toxicity of the fabricated PGS-PHB nanofibrous scaffold was also quantitatively evaluated by MTT assay when ADSCs cultured on the surface of the PGS-PHB nanofibers and TCP. The results demonstrated an increasing pattern over 10 days for both groups, and there was no significant difference between the two groups (Fig. 3E).

3.3. Osteogenic differentiation characterization

ALP activity of the cultured ADSCs on the fabricated PGS-PHB nanofibrous scaffold and TCP was evaluated as a critical osteogenic differentiation marker on days 7 and 14. The results revealed that ALP activity of the ADSCs cultured on the PGS-PHB nanofibrous scaffold was significantly higher than those ADSCs cultured on the TCP on both days. Mineralization due to the osteogenic differentiation is another important osteogenic-related marker that investigated qualitatively and quantitatively during the period of study. The results obtained by SEM demonstrated mineralization over the surface of the PGS-PHB nanofibers, however, these sediments also consist spherical calcium-containing mineral assemblages that seem to have a porous structure

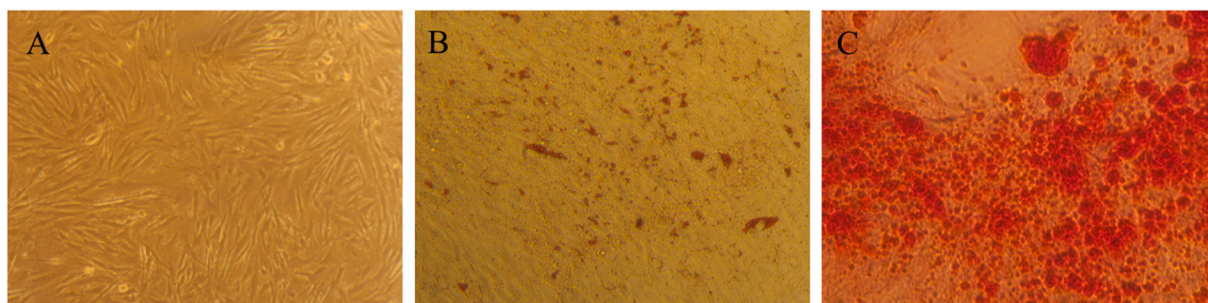


Fig. 1. Morphology of human adipose derived stem cells (ADSCs) cultured under basal medium (A), ADSCs cultured under adipogenic medium and then stained by oil red after two weeks (B) and ADSCs cultured under osteogenic medium for two weeks and stained by alizarin red (C). (For interpretation of the references to colour in this figure legend, the reader is referred to the Web version of this article.)

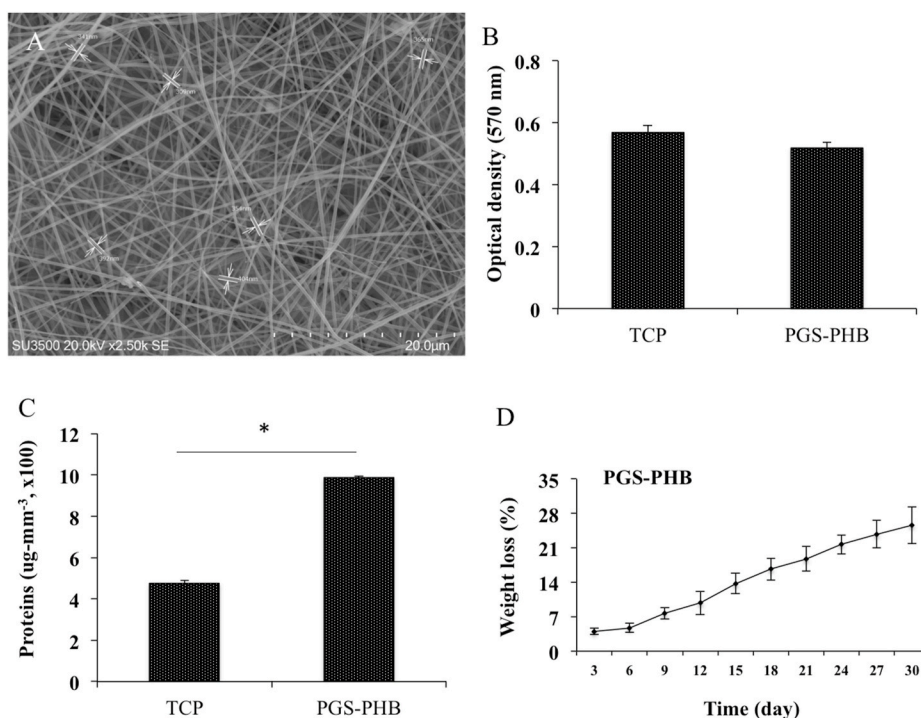


Fig. 2. SEM photograph of PGS-PHB nanofibrous scaffold (A). The results obtained from Cell attachment (B) and Protein adsorption (C) assays of PGS-PHB nanofibrous scaffold in comparison with TCP as a control. The results obtained from *In vitro* degradation assay of PGS-PHB nanofibrous scaffold during 30 days (D). The significant differences between groups are indicated with a star (* = $P < 0.05$).

(Fig. 4A). Total calcium secreted by ADSCs during the differentiation process was also measured on days 7 and 14. The results demonstrated that the amount of calcium measured in the PGS-PHB group was significantly higher than the TCP group on both days (Fig. 4B). For more detailed evaluation of the ADSCs osteogenic differentiation, five important bone-related genes were quantitatively evaluated in the ADSCs cultured in the PGS-PHB nanofibrous scaffold and TCP groups. The expression levels of Runx-2, ALP, Col-1, osteonectin and osteocalcin genes in the ADSCs cultured on the PGS-PHB nanofibrous scaffold were significantly higher than those cells cultured in the TCP group (Fig. 5).

4. Discussion

Due to the limitations faced with treating bone lesions, today, tissue-engineering specialists offer a wide variety of implants for treating this type of lesion [35–37]. Although in recent years tissue engineering has used a variety of synthetic and natural polymers to fabricate 3D scaffolds, efforts are still underway to introduce the most optimal scaffolds. The most important challenges facing these polymers are their

biodegradation rate and their structural affinity for the underlying bone matrix.

One of the most popular polymers in bone tissue engineering is a class of natural polyesters called PHAs [38]. Routine use of these polymers is in biomedical applications such as orthopedic pins, sutures, springs, etc. [20]. Among PHAs, PHB with its unique properties such as biocompatibility, biodegradability and piezoelectricity has shown high potential for use in bone tissue engineering [39]. The piezoelectric property of this polymer by itself can stimulate the growth of bone cells to regenerate and repair damaged bone tissue [40]. The most important disadvantage of fabricated scaffolds by this polymer is its poor mechanical properties, and to overcome this problem, the composite of this polymer can be used with other polymers [41].

In this study, for improvement of the PHB properties, it was composited with PGS. PGS is a polymer that has been introduced for use in tissue engineering, especially in soft tissues such as the cardiac, nerve and blood vessels. The mechanical and elastomeric properties of this polymer, along with the enzymatic and hydrolytic degradation of this polymer to completely non-toxic glycerol and sebacic acid molecules,

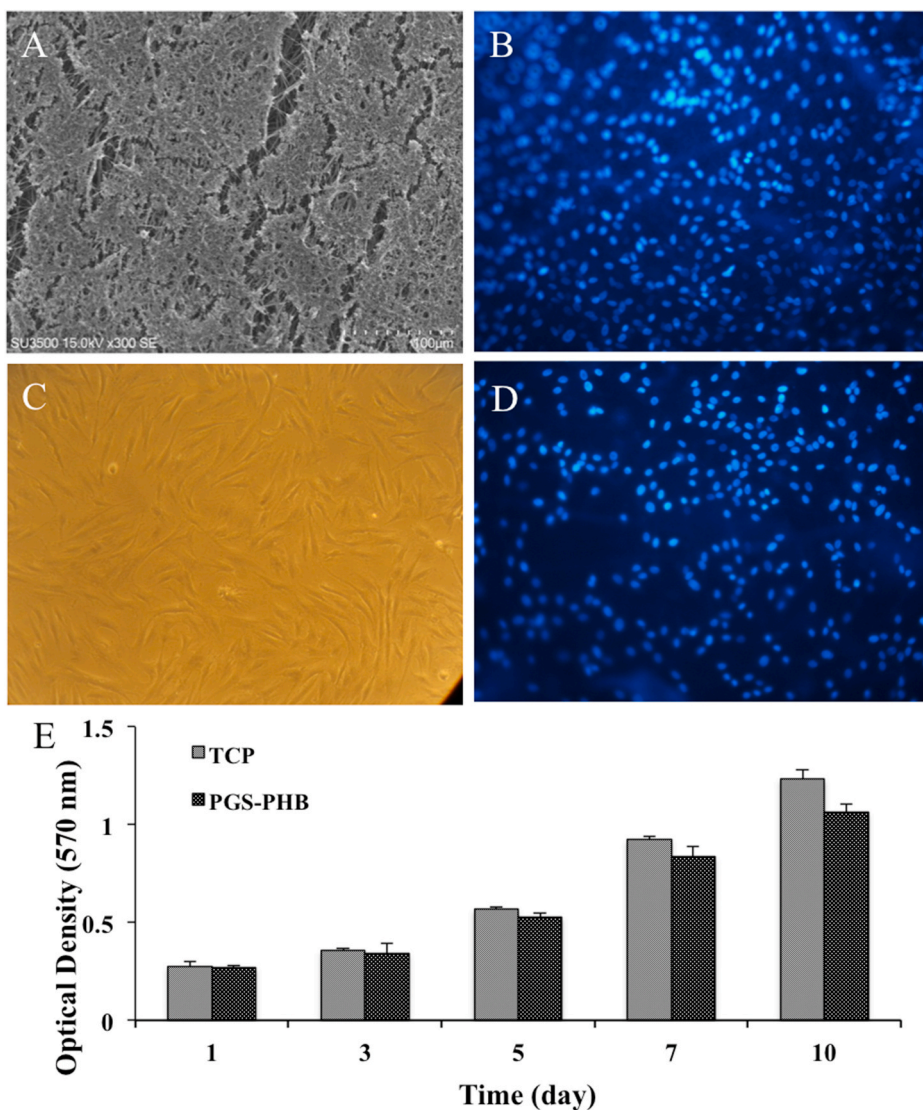


Fig. 3. Photographs of PGS-PHB nanofibrous scaffold 10 days after culture of human adipose derived stem cells (ADSCs) under basal medium depicted by SEM (A) and after DAPI staining depicted by florescent microscope (B). Photographs of ADSCs cultured TCP 10 days after cell seeding by light microscope (C) and after DAPI staining depicted by florescent microscope (D). Viability assessment of the ADSCs cultured on the PGS-PHB nanofibrous scaffold and TCP on days 1, 3, 5, 7 and 10 (E).

make it a very suitable option for use in tissue engineering [42]. The rationale behind the selection of PGS and PHB polymers was based on their mechanical, degradation and piezoelectric properties, given that these features are predicted to have positive effects on the stem cell attachment, proliferation and osteogenic differentiation.

PGS-PHB electrospun nanofibers were first structurally and morphologically evaluated using SEM. The results of this section showed that the fabricated scaffold contained fibers at the nanometer scale, without beads and uniform. The results showed also that the fabricated scaffold was very porous while the pores were interconnected to each other. It has been reported that, these pores help to anchor cells as well as intercellular connections [43]. Then, the biocompatibility of the fabricated scaffolds was evaluated using cell attachment, protein adsorption and cell survival tests. The results showed that the rate of cell adhesion and adsorbed protein in the constructed scaffold was significantly higher than the TCP group, which was considered as a control. Furthermore, the survival rate of cultured ADSCs on the scaffold and TCP was compared over a ten-day period. The results showed that ADSCs grew and survived properly on the surface of the PGS-PHB nanofibrous scaffolds while compared with the TCP group, indicating acceptable biocompatibility of the fabricated scaffold.

In agreeing with the results obtained in this study, Hu et al. were shown that the rat PC12 cell proliferation was increased when cultured on the PGS copolymers with poly methyl methacrylate (PMMA) (PGS-

PMMA) in comparison with the cells cultured on the TCP substrate during 8 days [44]. Yan et al. were also confirmed the cytocompatibility of the PLLA-PGS when A59 neuronal cells cultured on the PLLA composites with different concentrations of the PGS in comparison with the cells cultured on TCP as a control [45].

To evaluate the osteo-supportive capability of the PGS-PHB nanofibers, ALP activity test was performed while ADSCs cultured under osteogenic medium on the scaffold and TCP surfaces. ALP activity increases sharply in the early stages of bone differentiation [46], which in turn increases calcium deposition and also stimulates other bone factors. The results showed a significant increase in ALP activity of the cultured ADSCs on fabricated PGS-PHB nanofibrous scaffold compared to the TCP group.

Since calcium production and deposition is another important functional-factor in bone differentiation [47], the amount of calcium was assessed quantitatively by calcium content test and qualitatively by SEM. SEM images showed integrated calcium deposition in the scaffold group. Furthermore, the amount of total calcium production in the PGS-PHB scaffold group was significantly higher than the TCP group.

For more detailed study, the expression level of five important genes was evaluated in the bone differentiation process. The expression level of all genes in the ADSCs cultured on the PGS-PHB scaffold was significantly higher than the ADSCs cultured in the control group (TCP). The bone regeneration capacity of the elastomeric PGS alone and in

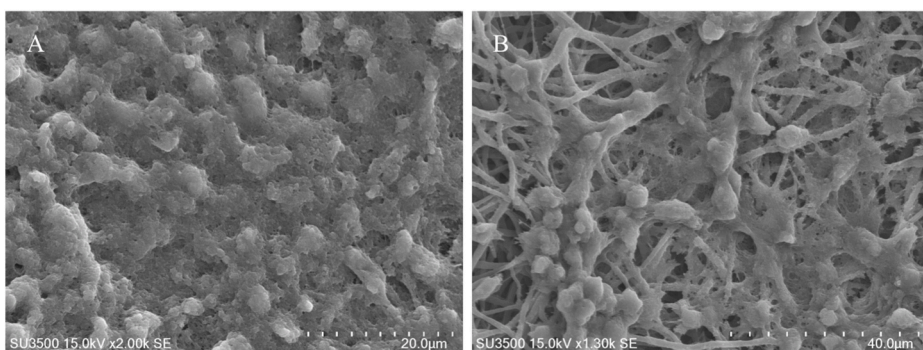


Fig. 4. SEM photograph of mineralization due to the osteogenic differentiation of human adipose derived stem cells (ADSCs) when cultured on PGS-PHB nanofibrous scaffold under osteogenic medium (A and B). Calcium (C) ALP activity (D) assessments of ADSCs cultured on PGS-PHB nanofibrous scaffold and TCP under osteogenic medium on days 7 and 14 (C). The significant differences between groups are indicated with a star (* = P < 0.05). The significant differences between groups are indicated with a star (* = P < 0.05).

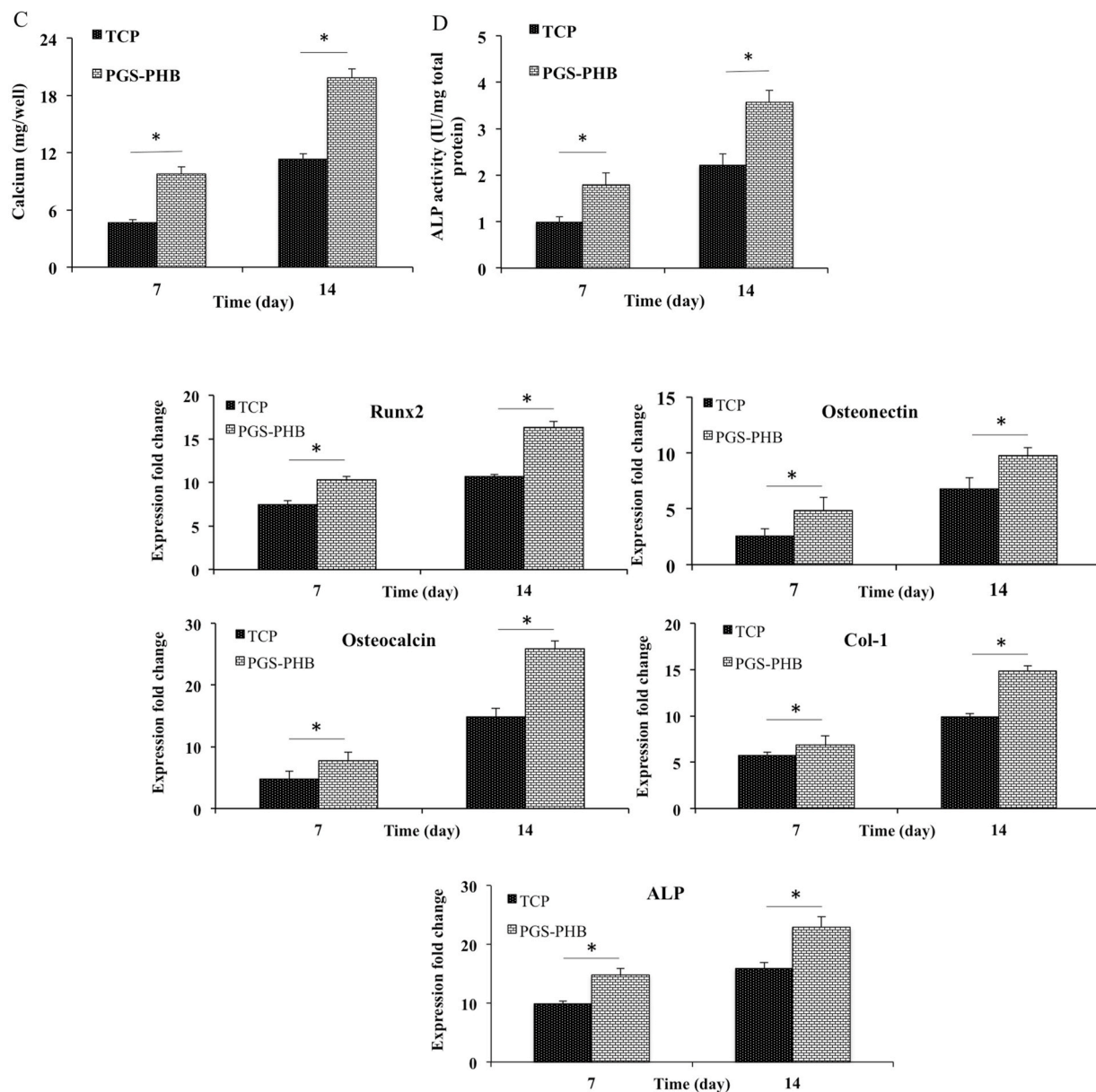


Fig. 5. Real time RT-PCR for bone-related genes during osteogenic differentiation of human adipose derived stem cells (ADSCs) when cultured on PGS-PHB nanofibrous scaffold and TCP under osteogenic medium on days 7 and 14. The significant differences between groups are indicated with a star (* = P < 0.05).

combination with HA particles and rabbit MSCs was reported previously by Zaky et al., while they implanted scaffolds in the ulna defect model in rabbits [29]. Their results revealed that PGS has a great bone regeneration property and this potential can significantly improve when MSCs cultured on the PGS scaffold. In another study, Jian et al., investigated

bone induction potential of the PGS microporous membranes (25 and 53 μm) and collagen membrane while implanted in the defect produced in the rabbit tibia [28]. Their results demonstrated that the 25 μm PGS membrane acted a valuable role in bone reconstruction compared to the other groups. Liang et al., was also reported that PGS scaffold

modification by grafting the adhesive ligands RGD and VEGF mimetic peptide can significantly improve MSCs viability during a week culture period [31]. In addition, they also showed that ALP activity and the expression level of ALP, Runx2 and osteonectin genes were increased significantly in the MSCs cultured on the PGS-RGD-VEGF compared to the cells cultured on the PGS or PGS-RGD scaffolds.

In a study conducted by Silva et al., PGS copolymer with PCL has been reported in cartilage tissue engineering [48]. In their study, human bone marrow derived MSCs were cultured on the Coaxial PGS-Kartogenin (KGN)/PCL nanofibers in comparison with PCL and PCL/PGS nanofibers without KGN. Their results demonstrated that those MSCs cultured on the PGS-KGN/PCL nanofibers under incomplete chondrogenic medium (without TGF- β 3) revealed the highest chondrogenic markers such as sGAG and cartilage-related gene markers compared to the other groups. It is well-known that collagen (types I, III, V) is the most important protein presence in the bone ECM, while type I (Col-I) contains more than 90% [49]. Therefore, scaffolds that can increase collagen production can also play a very important role in bone repair. As the results of gene expression had shown, the production of Col-I in the cells cultured on the PGS-PHB scaffolds were significantly increased compared to the control group. Jeffries et al. previously reported this potential of the PGS nanofibers when they compared collagen production capacity of the PLGA and PGS nanofibers after subcutaneously implanted in mice [50]. Their results demonstrated that collagen deposition detected by Masson's trichrome staining in the electrospun PGS nanofibers was almost similar to the PLGA nanofibers.

5. Conclusion

According to the results, electrospun PGS and PHB scaffold had a porous nanofibrous structure while being biocompatible. In addition, the osteogenic differentiation capacity of the ADSCs cultured on the PGS-PHB nanofibers was increased significantly compared to the ADSCs cultured on the TCP as a control group. It can be concluded that the PGS-PHB nanofibers have a great promising potential for use in bone and orthopedic tissue engineering applications.

Data sharing and data accessibility

The datasets used and/or analyzed during the current study are available from the corresponding author on reasonable request.

Conflict of competing interest

The authors (Mohammad Foad Abazari, Shohreh Zare Karizi, Hadi Samadian, Navid Nasiri, Hassan Askari, Matin Asghari, Fateme Frootan, Hadi Bakhtiari, Javad Hashemi, Vahid Mansouri) declare that they do not have a conflict of interest for the manuscript titled: Poly (glycerol sebacate) and Polyhydroxybutyrate electrospun nanocomposite facilitates osteogenic differentiation of mesenchymal stem cells, that submitted to the *journal of drug delivery science and technology*.

Author's contribution

Abazari M.F, Zare-Karizi S and Samadian H; performed the experiments, analyzed the data; Nasiri N, Askari H and Asghari M; did literature, designed the experiments, analyzed the data, and prepared the manuscript draft; Frootan F, Bakhtiari H and Mahboudi H; designed the scaffold fabrication and transduction methods; Mansouri V: funding, designed the experiments and approved the data and manuscript.

Declaration of competing interest

The authors declare that they do not have a conflict of interest.

References

- [1] N. Su, et al., Bone function, dysfunction and its role in diseases including critical illness, *Int. J. Biol. Sci.* 15 (4) (2019) 776.
- [2] T.A. Einhorn, L.C. Gerstenfeld, Fracture healing: mechanisms and interventions, *Nat. Rev. Rheumatol.* 11 (1) (2015) 45.
- [3] A. Oryan, S. Monazzah, A. Bigham-Sadegh, Bone injury and fracture healing biology, *Biomed. Environ. Sci.* 28 (1) (2015) 57–71.
- [4] P. Suchomel, et al., Autologous versus allogenic bone grafts in instrumented anterior cervical discectomy and fusion: a prospective study with respect to bone union pattern, *Eur. Spine J.* 13 (6) (2004) 510–515.
- [5] N.S. Moghaddam, et al., Metals for bone implants: safety, design, and efficacy, *Biomanufact. Rev.* 1 (1) (2016) 1–16.
- [6] F.R. Kloss, V. Offermanns, A. Kloss-Brandstätter, Comparison of allogeneic and autogenous bone grafts for augmentation of alveolar ridge defects—a 12-month retrospective radiographic evaluation, *Clin. Oral Implants Res.* 29 (11) (2018) 1163–1175.
- [7] D. Carluccio, et al., Challenges and opportunities in the selective laser melting of biodegradable metals for load-bearing bone scaffold applications, *Metall. Mater. Trans.* 51 (2020) 3311–3334.
- [8] S.L. Moradi, et al., Bone tissue engineering: adult stem cells in combination with electrospun nanofibrous scaffolds, *J. Cell. Physiol.* 233 (10) (2018) 6509–6522.
- [9] G.L. Koons, M. Diba, A.G. Mikos, Materials design for bone-tissue engineering, *Nat. Rev. Mater.* 5 (8) (2020) 584–603.
- [10] A. Mirzaei, et al., Synergistic effects of polyaniline and pulsed electromagnetic field to stem cell osteogenic differentiation on polyvinylidene fluoride scaffold, *Artificial Cells, Nanomed. Biotechnol.* 47 (1) (2019) 3058–3066.
- [11] A. Khademhosseini, R. Langer, A decade of progress in tissue engineering, *Nat. Protoc.* 11 (10) (2016) 1775–1781.
- [12] M. Izadpanahi, et al., Nanotopographical cues of electrospun PLLA efficiently modulate non-coding RNA network to osteogenic differentiation of mesenchymal stem cells during BMP signaling pathway, *Mater. Sci. Eng. C* 93 (2018) 686–703.
- [13] A. Mirzaei, et al., Comparison of osteogenic differentiation potential of induced pluripotent stem cells on 2D and 3D polyvinylidene fluoride scaffolds, *J. Cell. Physiol.* 234 (10) (2019) 17854–17862.
- [14] B. Guo, P.X. Ma, Synthetic biodegradable functional polymers for tissue engineering: a brief review, *Sci. China Chem.* 57 (4) (2014) 490–500.
- [15] P. Zhao, et al., Fabrication of scaffolds in tissue engineering: a review, *Front. Mech. Eng.* 13 (1) (2018) 107–119.
- [16] B. Dhandayuthapani, et al., Polymeric scaffolds in tissue engineering application: a review, *Int. J. Polym. Sci.* 2011 (2011) 1–19. <https://doi.org/10.1155/2011/290602>.
- [17] B. Bageshlooyafshar, et al., Zinc silicate mineral-coated scaffold improved in vitro osteogenic differentiation of equine adipose-derived mesenchymal stem cells, *Res. Vet. Sci.* 124 (2019) 444–451.
- [18] J. Chen, et al., Conductive nanofibrous composite scaffolds based on in-situ formed polyaniline nanoparticle and polylactide for bone regeneration, *J. Colloid Interface Sci.* 514 (2018) 517–527.
- [19] C. Utsunomia, Q. Ren, M. Zinn, Poly (4-hydroxybutyrate): current state and perspectives, *Front. Bioeng. Biotechnol.* 8 (2020) 257.
- [20] A.P. Bonartsev, et al., Application of polyhydroxyalkanoates in medicine and the biological activity of natural poly (3-hydroxybutyrate), *Acta Naturae (английская версия)* 11 (2) (2019), 41.
- [21] M.F. Abazari, et al., Curcumin-loaded PHB/PLLA Nanofibrous Scaffold Supports Osteogenesis in Adipose-derived Stem Cells in Vitro, *Polymers for Advanced Technologies*, 2021.
- [22] Y.S. Petronyuk, et al., Developing techniques of acoustic microscopy for monitoring processes of osteogenesis in regenerative medicine, *Bull. Russ. Acad. Sci. Phys.* 84 (6) (2020) 653–656.
- [23] E.I. Shishatskaya, I.A. Khlusov, T.G. Volova, A hybrid PHB–hydroxyapatite composite for biomedical application: production, in vitro and in vivo investigation, *J. Biomater. Sci. Polym. Ed.* 17 (5) (2006) 481–498.
- [24] M. Degli Esposti, et al., Highly porous PHB-based bioactive scaffolds for bone tissue engineering by in situ synthesis of hydroxyapatite, *Mater. Sci. Eng. C* 100 (2019) 286–296.
- [25] L. Liu, et al., Tricalcium phosphate sol-incorporated poly (ϵ -caprolactone) membrane with improved mechanical and osteoinductive activity as an artificial periosteum, *ACS Biomater. Sci. Eng.* 6 (8) (2020) 4631–4643.
- [26] R. Rai, et al., Synthesis, properties and biomedical applications of poly (glycerol sebacate)(PGS): a review, *Prog. Polym. Sci.* 37 (8) (2012) 1051–1078.
- [27] Y. Deng, et al., Repair of critical-sized bone defects with anti-miR-31-expressing bone marrow stromal stem cells and poly (glycerol sebacate) scaffolds, *Eur. Cell. Mater.* 27 (1) (2014).
- [28] B. Jian, et al., Microporous elastomeric membranes fabricated with polyglycerol sebacate improved guided bone regeneration in a rabbit model, *Int. J. Nanomed.* 14 (2019) 2683.
- [29] S.H. Zaky, et al., Poly (glycerol sebacate) elastomer: a novel material for mechanically loaded bone regeneration, *Tissue Eng.* 20 (1–2) (2014) 45–53.
- [30] Y. Ma, et al., PEGylated poly (glycerol sebacate)-modified calcium phosphate scaffolds with desirable mechanical behavior and enhanced osteogenic capacity, *Acta Biomater.* 44 (2016) 110–124.
- [31] B. Liang, et al., Poly (glycerol sebacate)-based bio-artificial multiporous matrix for bone regeneration, *Front. Chem.* 8 (2020).
- [32] J. Varshosaz, et al., Rapid hemostasis by nanofibers of polyhydroxyethyl methacrylate/polyglycerol sebacic acid: an in vitro/in vivo study, *J. Appl. Polym. Sci.* 138 (5) (2021) 49785.

- [33] E. Saburi, et al., Bone morphogenetic protein-7 incorporated polycaprolactone scaffold has a great potential to improve survival and proliferation rate of the human embryonic kidney cells, *J. Cell. Biochem.* 120 (6) (2019) 9859–9868.
- [34] A. Ardeshiryajimi, et al., Comparison of osteogenic differentiation potential of human adult stem cells loaded on bioceramic-coated electrospun poly (L-lactide) nanofibres, *Cell Prolif* 48 (1) (2015) 47–58.
- [35] J.R. Perez, et al., Tissue engineering and cell-based therapies for fractures and bone defects, *Front. Bioeng. Biotechnol.* 6 (2018) 105.
- [36] X. Du, S. Fu, Y. Zhu, 3D printing of ceramic-based scaffolds for bone tissue engineering: an overview, *J. Mater. Chem. B* 6 (27) (2018) 4397–4412.
- [37] L. Roseti, et al., Scaffolds for bone tissue engineering: state of the art and new perspectives, *Mater. Sci. Eng. C* 78 (2017) 1246–1262.
- [38] J. Lim, et al., Emerging bone tissue engineering via Polyhydroxyalkanoate (PHA)-based scaffolds, *Mater. Sci. Eng. C* 79 (2017) 917–929.
- [39] R. Dwivedi, et al., Poly hydroxyalkanoates (PHA): role in bone scaffolds, *J. Oral Biol. Craniofacial Resear.* 10 (1) (2020) 389–392.
- [40] J. Jacob, et al., Piezoelectric smart biomaterials for bone and cartilage tissue engineering, *Inflamm. Regen.* 38 (1) (2018) 1–11.
- [41] A. El-Hadi, et al., Correlation between degree of crystallinity, morphology, glass temperature, mechanical properties and biodegradation of poly (3-hydroxyalkanoate) PHAs and their blends, *Polym. Test.* 21 (6) (2002) 665–674.
- [42] M. Gultekinoglu, et al., Preparation of poly (glycerol sebacate) fibers for tissue engineering applications, *Eur. Polym. J.* 121 (2019) 109297.
- [43] J. Venugopal, et al., Interaction of cells and nanofiber scaffolds in tissue engineering, *J. Biomed. Mater. Res. B Appl. Biomater.* 84 (1) (2008) 34–48.
- [44] J. Hu, et al., Electrospinning of poly (glycerol sebacate)-based nanofibers for nerve tissue engineering, *Mater. Sci. Eng. C* 70 (2017) 1089–1094.
- [45] Y. Yan, et al., Tailoring the wettability and mechanical properties of electrospun poly (l-lactic acid)-poly (glycerol sebacate) core-shell membranes for biomedical applications, *J. Colloid Interface Sci.* 508 (2017) 87–94.
- [46] A. Rutkovskiy, K.-O. Stensløkken, I.J. Vaage, Osteoblast differentiation at a glance, *Medical Sci. Monitor Basic Resear.* 22 (2016) 95.
- [47] P.H. Schlesinger, et al., Cellular and extracellular matrix of bone, with principles of synthesis and dependency of mineral deposition on cell membrane transport, *Am. J. Physiol. Cell Physiol.* 318 (1) (2020) C111–C124.
- [48] J.C. Silva, et al., Kartogenin-loaded coaxial PGS/PCL aligned nanofibers for cartilage tissue engineering, *Mater. Sci. Eng. C* 107 (2020) 110291.
- [49] X. Lin, et al., The bone extracellular matrix in bone formation and regeneration, *Front. Pharmacol.* (2020) 11.
- [50] E.M. Jeffries, et al., Highly elastic and suturable electrospun poly (glycerol sebacate) fibrous scaffolds, *Acta Biomater.* 18 (2015) 30–39.